BULLETIN OF THE POLISH ACADEMY OF SCIENCES
TECHNICAL SCIENCES, Vol. 60, No. 4, 2012
DOI: 10.2478/v10175-012-0091-9

VARIA

Numerical simulations of acoustic waves with the graphic acceleration GAMER code

K. MURAWSKI[1]*, K. MURAWSKI, Jr.[2], and H.-Y. SCHIVE[3]

[1] Faculty of Physics, Mathematics and Informatics, University of Maria Curie-Skłodowska, 1 M. Curie-Skłodowskiej Sq., 20-031 Lublin, Poland
[2] Institute of Informatics, University of Maria Curie-Skłodowska, 1 M. Curie-Skłodowskiej Sq., 20-031 Lublin, Poland
[3] Department of Physics, National Taiwan University, 10617, Taipei, Taiwan

Abstract. We present results of numerical simulations of acoustic waves with the use of the Graphics Processing Unit (GPU) acceleration GAMER code which implements a second-order Godunov-type numerical scheme and adaptive mesh refinement (AMR). The AMR implementation is based on constructing a hierarchy of grid patches with an octree data structure. In this code a hybrid model is adopted, in which the time-consuming solvers are dealt with GPUs and the complex AMR data structure is manipulated by Central Processing Units (CPUs). The code is highly parallelized with the Hilbert space-filling curve method. These implementations allow us to resolve well desperate spatial scales that are associated with acoustic waves. We show that a localized velocity (gas pressure) pulse that is initially launched within a uniform and still medium triggers acoustic waves simultaneously with a vortex (an entropy mode). In a flowing medium, acoustic waves experience amplitude growth or decay, a scenario which depends on a location of the flow and relative direction of wave propagation. The amplitude growth results from instabilities which are associated with negative energy waves.

Key words: numerical simulation, acoustic waves, graphic acceleration GAMER code.

1. Introduction

Most of natural phenomena are so complex that they can be described by mathematical equations, which cannot in general be solved analytically and require numerical treatment. A typical way of this treatment is to transform these equations to a discrete form that can be numerically dealt with. In this way, the initial state of a system is established and subsequent events are evaluated. The continuous interaction with experiments, observations and analysis results in numerical simulations attaining a status of an indispensable tool of research. As a result, the increase in computing power as well as in capacity of numerical algorithms is vital in obtaining good quality solutions. This increase can be gained with the use of many cores and accelerator-based programming which recently became promising techniques in high-performance computing. Among others, Graphics Processing Units (GPUs) for acceleration of numerical calculations acquired a potential attention in the past few years. However, the original purpose of GPU is to serve as an accelerator for computer graphics. The modern GPU, for instance the NVIDIA Tesla C2075, has 448 scalar processor cores, also called CUDA cores, each working at 1.15 GHz clock rate. It delivers a peak performance of 1,030 GFLOPS (Giga Floating Operations Per Second) in single precision calculations and 515 GFLOPS in double precision calculations, which is about an order of magnitude higher than the modern CPUs. In addition, it has 6 GB of GDDR5 memory with a bandwidth of 144 GB/s. The 448 scalar processor cores are grouped into 14 multiprocessors, each of which consists of 32 scalar processor cores and shares a 48 kB on-chip data cache.

The traditional GPU scheme adopts the high-level shading languages, which are designed for graphic rendering and require knowledge of computer graphics. As a result, its use is cumbersome and it is unsuitable for general-purpose computations. User-friendly programming interfaces of GPU for general-purpose usage have been developed since 2006. The most popular interfaces include the Compute Unified Device Architecture (CUDA) [1], and the Open Computing Language (OpenCL) [2]. The latter is a cross-platform Application Programming Interface (API), which is devoted for heterogeneous systems, including GPU, CPU, FPGA (Field Programmable Gate Array), Intel MIC (Many Integrated Core), and IBM's Cell processor. Here we concentrate on CUDA which is adopted in the GAMER code [3, 4] and in which GPU is regarded as a multi-threaded coprocessor to CPU with a standard C language interface. To define the computational task for GPU, programmers should provide a C-like function called kernel, which can be executed by multiple CUDA threads in parallel.

A goal of this paper is to adopt the graphic accelerated GAMER code for solving initial-value problem of Euler equations which describe acoustic waves. These equations are introduced in Sec. 2. Numerical simulations with the use of the GAMER code are presented in Sec. 3. Results of these simulations for acoustic waves are illustrated in Sec. 4. This paper is completed by summary of main results.

*e-mail: kmur@kft.umcs.lublin.pl

2. Euler equations

We consider here Euler equations in the conservation form:

$$\frac{\partial \varrho}{\partial t} + \nabla \cdot (\varrho \mathbf{V}) = 0, \tag{1}$$

$$\frac{\partial (\varrho \mathbf{V})}{\partial t} + \nabla \cdot (\varrho \mathbf{V}\mathbf{V}) = -\nabla p, \tag{2}$$

$$\frac{\partial E}{\partial t} + \nabla \cdot [(E+p)\mathbf{V}] = 0. \tag{3}$$

Here ϱ is the mass density, p is the gas pressure, $\mathbf{V} = [V_\mathrm{x}, V_\mathrm{y}, V_\mathrm{z}]$ is the flow velocity,

$$E = \frac{1}{2}\varrho \mathbf{V}^2 + \frac{p}{\gamma - 1} \tag{4}$$

is total (kinetic plus internal) energy density and γ is the adiabatic index which we set and hold fixed to $\gamma = 5/3$.

3. Numerical simulations with the GAMER code

The numerical simulations in this paper are performed with the use of the newly developed adaptive mesh refinement *GAMER* code [3, 4], which implements a second-order unsplit Godunov solver [5–7].

To initiate a fluid condition we set the simulation box as $0 \le x \le 20$ Mm $\times$ $0 \le y \le 20$ Mm $\times$ $0 \le z \le 20$ Mm and adopt periodic boundary conditions at all boundary surfaces of the simulation box. Here $1\,\mathrm{Mm} = 10^6\,\mathrm{m}$. Setting these periodic conditions is currently the only option in GAMER. The computational domain is first covered by root patches of the cuboid shape with the lowest spatial resolution. Then, according to the user-defined refinement criteria, each root patch may be refined into eight child patches with a spatial resolution twice that of their parent patch. The numerical solutions in different patches are calculated simultaneously by multiple processors inside GPUs. In our studies, we use the AMR grid with a minimum (maximum) level of refinement blocks set to 0 (5). The refinement strategy is based on controlling numerical errors in either a fluid quantity or its gradient. Depending on the context, we use as this quantity either flow velocity, gas pressure, mass density or both. These settings lead to excellent resolution of dramatic spatial profiles, which significantly reduce the numerical diffusion within the simulation region.

The main aim of developing GAMER is to highly improve the simulation performance with GPU acceleration. In AMR simulations, generally the most time-consuming part is to solve the fluid equations patch by patch. A hybrid CPU/GPU model is adopted in the code, in which the fluid solvers are implemented into GPU and the complicated AMR data structure is manipulated by CPU [3]. CPU and GPU are allowed to work concurrently, which improves the overall performance further. Additionally, a hybrid OpenMP/MPI/GPU parallelization model has been implemented in order to fully optimize the performance in heterogeneous CPU+GPU clusters [4], and the Hilbert space-filling curve is adopted to improve load balance. This code features an extraordinary performance by taking advantage of the GPU acceleration. GPU is a highly parallel multi-threaded coprocessor to CPU, which typically has hundreds of processors working in a single-instruction multiple-thread fashion. Most importantly, up to two orders of magnitude performance speed-up has been demonstrated in comparison with CPU-only computation [4]. The code is able to solve the Euler equations with self-gravity [3] but in this paper we limit ourselves to a gravity-free case that corresponds to Eqs. (1)–(3).

4. Results of numerical simulations

In this part of the paper we present the results of numerical simulations we performed with the use of the GAMER code. We discuss the cases of still and moving equilibria separately in the following subsections.

4.1. The case of a still equilibrium. We consider first the fluid at its equilibrium state which is described by uniform quantities with the subscript $_0$ as

$$\varrho_0, \quad \mathbf{V}_0 = \mathbf{0}, \quad p_0 = \frac{1}{\gamma}\varrho_0 c_\mathrm{s}^2. \tag{5}$$

Here $c_\mathrm{s} = \sqrt{\gamma p_0/\varrho_0}$ is the sound speed which we set and hold fixed as $c_\mathrm{s} = 0.2$ Mm s^{-1} as well as $\varrho_0 = 10^{-12}$ kg m^{-3}. Although these values are characteristic to the solar corona their exact values are not important as they do not influence the general scenario of fluid evolution.

Excitation of a vortex by a localized velocity pulse. We excite waves in the aforementioned uniform and still medium of Eq. (5) by launching initially, at $t = 0$ s, the impulse in a y component of velocity V_y, i.e.

$$V_\mathrm{y}(x, y, z, t = 0) = A_\mathrm{V} \exp\left[-\frac{(x-x_0)^2 + (y-y_0)^2 + (z-z_0)^2}{w^2}\right]. \tag{6}$$

Here A_V is the amplitude of the initial Gaussian pulse, (x_0, y_0, z_0) its initial position, and w its width. We set and hold fixed $w = 0.25$ Mm, $A_\mathrm{V} = 0.2\,c_\mathrm{s}$, and $x_0 = y_0 = z_0 = 5$ Mm.

Figure 1 illustrates the spatial profiles of the mass density $\varrho(x, y, z = z_0)$, and velocity vectors at $t = 2$ s and $t = 20$ s. The initial pulse separates in its usual way into counter-propagating waves, which can be clearly seen at $t = 2$ s (top). As the fluid is initially pushed upwards it becomes compressed (rarefied) at the top (bottom). These compressed and rarefied regions are located at ($x = 5$ Mm, $y = 5.5$ Mm) and ($x = 5$ Mm, $y = 4.5$ Mm) and they correspond respectively to the red and blue patches in Fig. 1. Note that a velocity pulse breaks a spatial symmetry of the fluid and as a result the waves propagating along the y-direction experience higher amplitudes than those propagating along the perpendicular (x- and z-) directions. This is particularly well seen at the initial stages of wave evolution (Fig. 1, top).

As a result of the action of the initial perturbation the fluid starts rotating in the form of a vortex, which is well seen at $t = 20$ s (Fig. 1, bottom). Such scenario results from the

fact that the hydrodynamic equations include both vortex and acoustic solutions [8, 9]. This vortex is associated with fluid depletion at the center of the vortex which exhibits a modified toroidal shape. Note that as a consequence of the initial momentum this vortex is slightly pushed upwards along the y-axis.

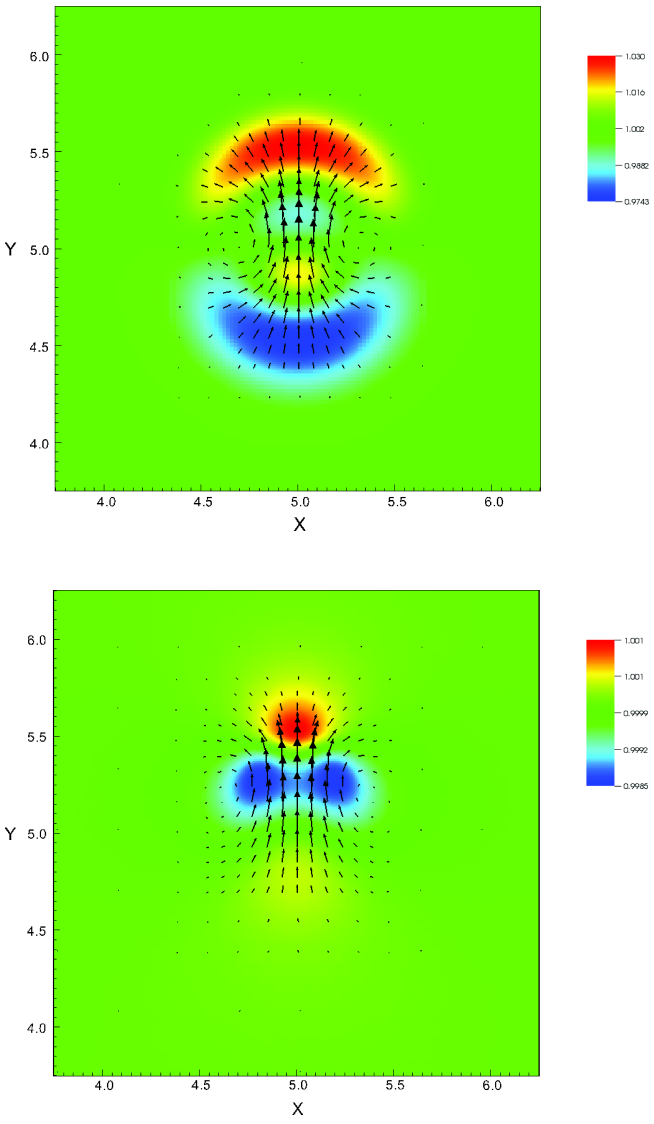

Fig. 1. Mass density $\varrho(x, y, z = z_0)$ (colour maps) and velocity vectors (arrows) profiles at $t = 2$ s (top) and $t = 20$ s (bottom) for the case of $A_{\rm V} = 0.2\, c_{\rm s}$ and still medium

Acoustic waves which are triggered by the initial pulse of Eq. (6) propagate away of the launching place. They can be well traced on the profiles of $V_{\rm y}(x = x_0, y, z = z_0)$. At $t = 10$ s these waves can be found at $y = 3$ Mm and $y = 7$ Mm (Fig. 2, top) and at $t = 20$ s these waves are at $y = 1$ Mm and $y = 9$ Mm (Fig. 2, bottom). Note that at $t = 10$ s the maximum of $V_{\rm y}(x = x_0, y, z = z_0)$ is located at $y \simeq 5.1$ Mm (Fig. 2, top), while at $t = 20$ s it is at $y \simeq 5.4$ Mm (Fig. 2, bottom).

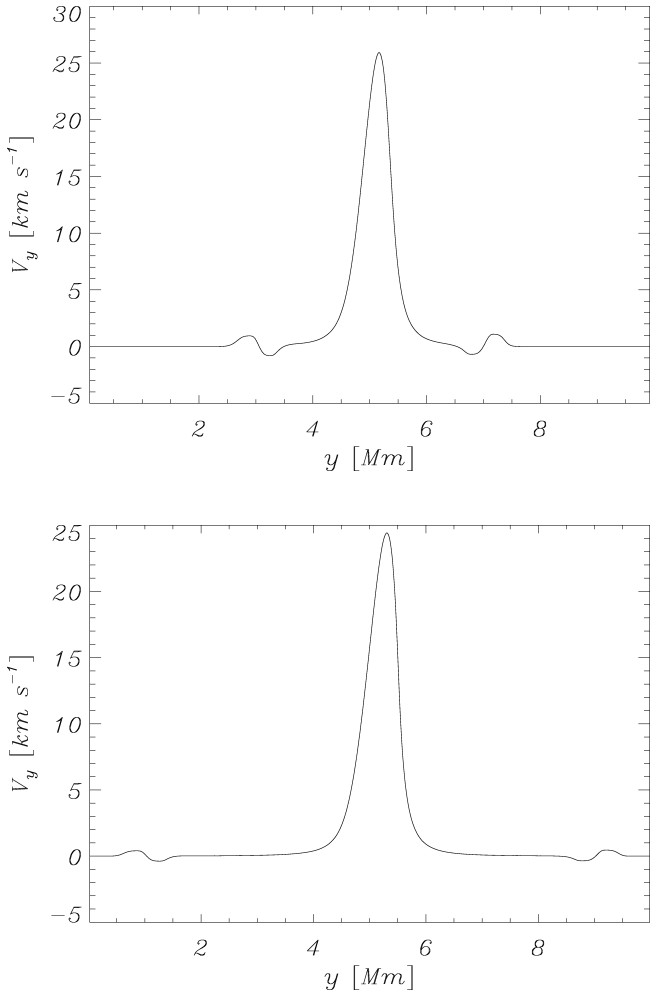

Fig. 2. Velocity $V_{\rm y}(x = x_0, y, z = z_0)$ profiles at $t = 10$ s (top) and $t = 20$ s (bottom) for the case of $A_{\rm p} = 0.2\, c_{\rm s}$, uniform and still medium

Excitation of the entropy mode by a pulse in a gas pressure. In this section we discuss waves which are impulsively excited in the uniform medium of Eq. (5) by launching initially, at $t = 0$ s, the Gaussian pulse in a gas pressure, i.e.

$$p(x, y, z, t = 0) = A_{\rm p} \exp\left[-\frac{(x - x_0)^2 + (y - y_0)^2 + (z - z_0)^2}{w^2}\right]. \quad (7)$$

Here $A_{\rm p} = 0.2\, p_0$ is the amplitude of the pulse. This initial pulse pushes the fluid out of the launching place which results in acoustic waves and fluid evacuation at the center of the initial pulse. These acoustic waves are well seen at $t = 2$ s and they are represented by velocity vectors (Fig. 3, top). The rarefied fluid region is represented by the blue patch that is located at the launching place. Surprisingly enough, this rarefied fluid does not evolve any more in time (Fig. 3, bottom) and the fluid attains new equilibrium with all other fluid quantities remaining flat at this point. This scenario is associated with the entropy mode which was recently discussed in the context of magnetized fluid by [10].

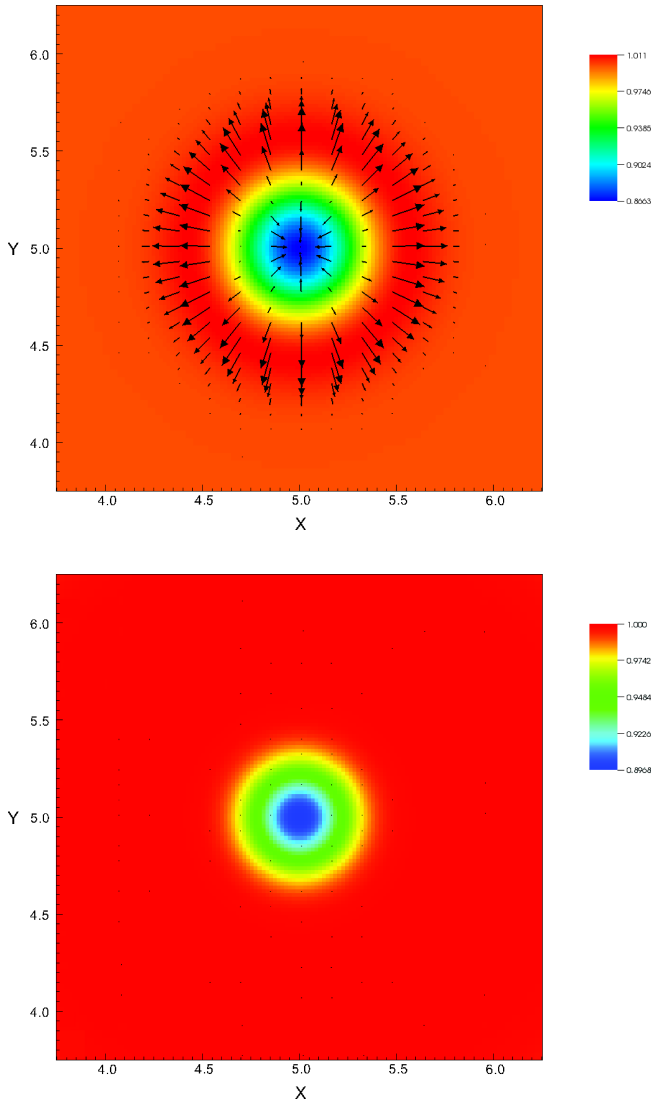

Fig. 3. Mass density $\varrho(x, y, z = z_0)$ (colour maps) and velocity vectors (arrows) profiles at $t = 2$ s (top) and $t = 10$ s (bottom) for the case of $A_\mathrm{p} = 0.2\, p_0$ and still medium

Figure 4 illustrates mass density evaluated for $x = z = 5$ Mm. Acoustic waves propagating away from the launching place, $y = 5$ Mm, are well seen; for $t = 10$ s these waves are at $y = 3$ Mm and $y = 7$ Mm (left) and for $t = 20$ s these waves are at $y = 1$ Mm and $y = 9$ Mm (right). The depression in a mass density, $\varrho(x_0, y_0, z_0) \simeq 0.9\varrho_0$, corresponds to the entropy mode which remains still at $y = y_0 = 5$ Mm.

Note that a case of $A_\mathrm{p} < 0$ results in acoustic waves propagation and the entropy mode which corresponds to a region of mass density enhancement rather than rarefaction (not shown).

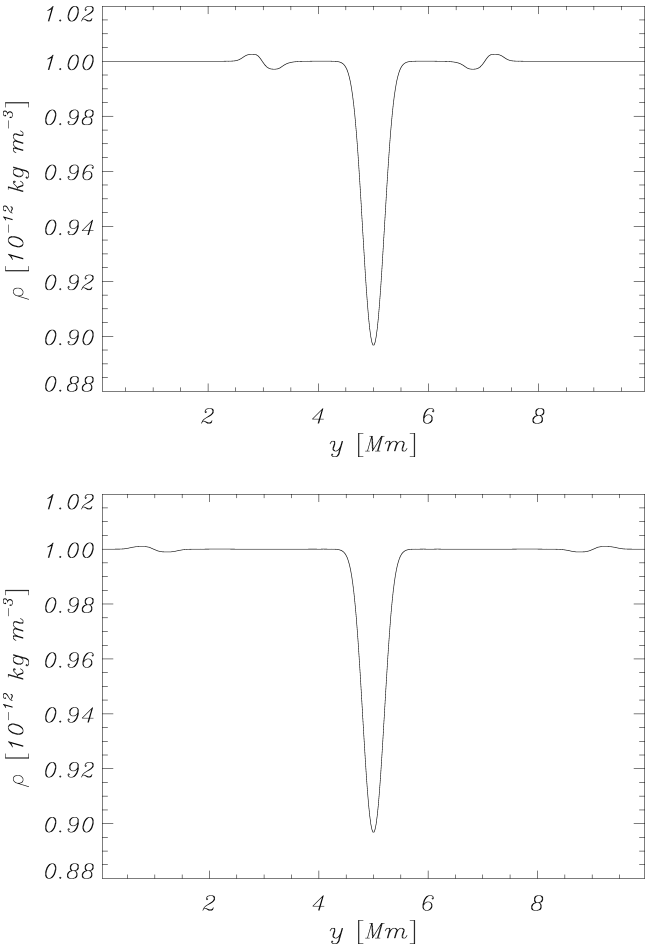

Fig. 4. Mass density $\varrho(x = x_0, y, z = z_0)$ profiles at $t = 10$ s (left) and $t = 20$ s (right) for the case of $A_\mathrm{p} = 0.2\, p_0$ and still medium

4.2. The case of a moving equilibrium. In this part of the paper we consider a fluid which moves along the y-direction in otherwise uniform medium, that is

$$\varrho_0 = 2 \cdot 10^{-12} \frac{\mathrm{kg}}{\mathrm{m}^3}, \quad p_0 = \frac{1}{\gamma} \varrho_0 c_\mathrm{s}^2, \tag{8}$$

$$\mathbf{V}_0 = \left[0, V_\mathrm{e} + (V_\mathrm{i} - V_\mathrm{e}) \mathrm{sech}^2 \frac{\sqrt{(x - x_\mathrm{l})^2 + (z - z_\mathrm{l})^2}}{a}, 0\right]. \tag{9}$$

Here x_l and z_l are coordinates of the center of the flow region, a is its width, V_i and V_e are magnitudes of the flow within the center and in the ambient medium, respectively. We set and hold fixed $x_\mathrm{l} = z_\mathrm{l} = 2.5$ Mm, $a = 0.5$ Mm, and discuss two cases: (a) $V_\mathrm{i} = 0.4\, c_\mathrm{s}$, $V_\mathrm{e} = 0$; (b) $V_\mathrm{i} = 0$, $V_\mathrm{e} = 0.4\, c_\mathrm{s}$. Acoustic waves and the entropy mode are triggered in these cases by the initial pulse in a gas pressure. See Eq. (7).

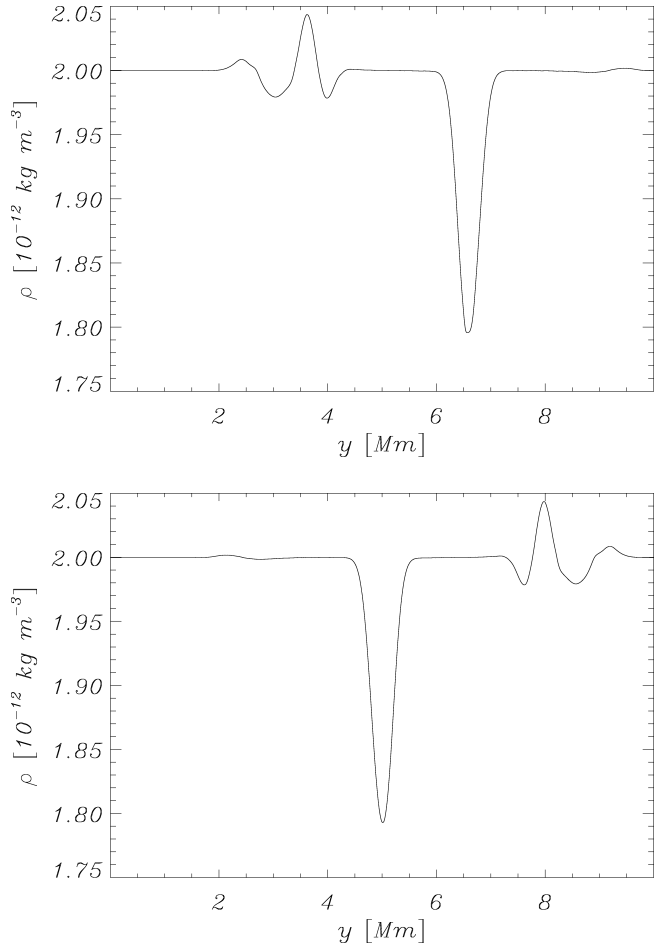

Fig. 5. Mass density $\varrho(x = x_1, y, z = z_1)$ profiles at $t = 20$ s for $A_\mathrm{p} = 0.2\,p_0$, $V_\mathrm{i} = 0.4\,c_\mathrm{s}$, $V_\mathrm{e} = 0$ (top) and $V_\mathrm{i} = 0$, $V_\mathrm{e} = 0.4\,c_\mathrm{s}$ (bottom)

Figure 5 illustrates the profiles of mass density, $\varrho(x = x_1, y, z = z_1)$, that results from the initial pulse of Eq. (7) with $A_\mathrm{p} = 0.2\,p_0$. In the case of (a) left-propagating (right-propagating) waves experience amplitude growth (decline), while in the case of (b) this scenario is reversed as right-propagating (left-propagating) waves exhibit amplitude enhancement (decay). This peculiar behavior of acoustic waves results from negative energy waves (NEW) instabilities for which wave amplitude grows when the energy of the flow and the wave is reduced in a presence of any dissipative effect. In our case dissipative effects result from numerical diffusion which is inherently present in any numerical system. For such NEW the instability condition

$$\omega \frac{\partial D}{\partial \omega} < 0, \tag{10}$$

has to be satisfied [11]. Here ω is a wave cyclic frequency and D represents the left-hand side of the dispersion relation, $D(\omega, k) = 0$ with k denoting a wavenumber. In our case we have [12]

$$D(\omega, k) = \Omega_\mathrm{i}^2 m_\mathrm{e} \frac{K_0'(m_\mathrm{e} a)}{K_0(m_\mathrm{e} a)} - \Omega_\mathrm{e}^2 m_\mathrm{i} \frac{I_0'(m_\mathrm{i} a)}{I_0(m_\mathrm{i} a)}, \tag{11}$$

where I_0 (K_0) is the (modified) Bessel function of order 0, $'$ denotes the partial derivative with respect to the argument of the function, and

$$m_\mathrm{i}^2 = \frac{k^2 c_\mathrm{s}^2 - \Omega_\mathrm{i}^2}{c_\mathrm{s}^2}, \qquad m_\mathrm{e}^2 = \frac{k^2 c_\mathrm{s}^2 - \Omega_\mathrm{e}^2}{c_\mathrm{s}^2}, \tag{12}$$

$$\Omega_\mathrm{i} = \omega + V_\mathrm{i} k, \qquad \Omega_\mathrm{e} = \omega + V_\mathrm{e} k. \tag{13}$$

In the case of (a) NEW occur for waves propagating towards negative values of y, while for (b) NEW result for waves propagating according to the direction of the y-axis [13], in agreement with our numerical findings.

5. Summary

In this paper we demonstrated a performance of the graphic accelerated GAMER code for acoustic waves which are described by the Euler equations. We presented a numerical study of the propagation of the acoustic waves in still and flowing media. The main findings can be summarized as follows. A localized pulse that is initially launched in a fluid velocity triggers acoustic waves and a vortex which stagnates the mass density around the launching place. An initial pressure pulse results in acoustic wave propagation as well. However, in this case no vortex is generated. Instead, the entropy mode settles in at the place the initial pulse was excited. This entropy mode corresponds to a region of permanent rarefaction or condensation, depending upon positive or negative perturbation in a gas pressure.

A flowing fluid breaks a symmetry of left- and rightwardly propagating waves. This asymmetry results from negative energy waves which occur for back-wardly propagating waves and which experience amplitude grow by extracting the corresponding energy from the fluid flow.

The numerical models we build on the bases of the GAMER code demonstrate the feasibility of fluid simulations in obtaining quantitative features of complex flows with fine spatial structures. These structures were finely resolved by the adaptation of sophisticated numerical methods such as shock-capturing scheme and adaptive mesh refinement.

These numerical simulations have been performed on nVidia Quadro FX 880M. A typical time of simulations was within the range of 15-30 min.

This work has been supported by a Marie Curie International Research Staff Exchange Scheme Fellowship within the 7th European Community Framework Program (K.M. and K.M., Jr.).

REFERENCES

[1] NVIDIA, *NVIDIA CUDA C Programming Guide (Version 4.1)*, Santa Clara, CA, NVIDIA, 2012.

[2] Khronos Group, *The OpenCL Specification (Version 1.2)*, Beaverton, OR, Khronos Group, 2011.

[3] H. Schive, Y. Tsai, and T. Chiueh, "GAMER: a graphic processing unit accelerated adaptive-mesh-refinement code for astrophysics", *Astrophys. J. Suppl.* 186, 457–484 (2010).

[4] H. Schive, U. Zhang, and T. Chiueh, "Directionally unsplit hydrodynamic schemes with hybrid MPI/OpenMP/GPU parallelization in AMR", CD-ROM arXiv 1103.3373(2011).

[5] S.K. Godunov, "A difference scheme for numerical solution of discontinuous solution of hydrodynamic equations", *Math. Sb.* 47, 271–306, (1959).

[6] K. Murawski Jr., K. Murawski, and P. Stpiczyński, "Implementation of MUSCL-Hancock method into the C++ code for the Euler equations", *Bull. Pol. Ac.: Tech.* 60 (1), 45–53 (2012).

[7] K. Murawski, D. Lee, "Numerical methods of solving equations of hydrodynamics from perspectives of the code FLASH", *Bull. Pol. Ac.: Tech.* 59 (1), 81–91 (2011).

[8] J. Lighthill, *Waves in Fluids*, Cambridge University Press, Cambridge, 1978.

[9] D.J. Acheson, *Elementary Fluid Dynamics*, Oxford University Press, New York, 1990.

[10] K. Murawski, T.V. Zaqarashvili, and V.M. Nakariakov, "Entropy mode at a magnetic null point as a possible tool for indirect observation of nanoflares in the solar corona", *Astron. Astrophys.* 533, A18 1–5 (2011).

[11] R.A. Cairns, "The role of negative energy waves in some instabilities of parallel flows", *J. Fluid Mech.* 92, 1–14 (1979).

[12] M. Terra-Homem, R. Erdelyi, and I. Ballai, "Linear and nonlinear MHD wave propagation in steady-state magnetic cylinders", *Solar Physics* 217, 199–223 (2003).

[13] P.S. Joarder, V.M. Nakariakov, and B. Roberts, "A manifestation of negative energy waves in the solar atmosphere", *Solar Physics* 176, 285–297 (1997).